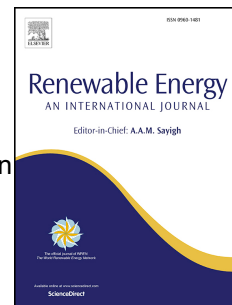


# Accepted Manuscript

A novel beta parameter based fuzzy-logic controller for photovoltaic MPPT application

Xingshuo Li, Huiqing Wen, Yihua Hu, Lin Jiang



PII: S0960-1481(18)30723-7

DOI: [10.1016/j.renene.2018.06.071](https://doi.org/10.1016/j.renene.2018.06.071)

Reference: RENE 10227

To appear in: *Renewable Energy*

Received Date: 8 January 2018

Revised Date: 28 May 2018

Accepted Date: 18 June 2018

Please cite this article as: Li X, Wen H, Hu Y, Jiang L, A novel beta parameter based fuzzy-logic controller for photovoltaic MPPT application, *Renewable Energy* (2018), doi: 10.1016/j.renene.2018.06.071.

This is a PDF file of an unedited manuscript that has been accepted for publication. As a service to our customers we are providing this early version of the manuscript. The manuscript will undergo copyediting, typesetting, and review of the resulting proof before it is published in its final form. Please note that during the production process errors may be discovered which could affect the content, and all legal disclaimers that apply to the journal pertain.

# A Novel Beta Parameter Based Fuzzy-Logic Controller for Photovoltaic MPPT Application

Xingshuo Li<sup>a,b</sup>, Huiqing Wen<sup>a,\*</sup>, Yihua Hu<sup>b</sup>, Lin Jiang<sup>b</sup>

<sup>a</sup>*Department of Electrical and Electronic Engineering, Xi'an Jiaotong-Liverpool University, Suzhou 215123, China*

<sup>b</sup>*Department of Electrical Engineering and Electronics, University of Liverpool, Liverpool L69 3GJ, United Kingdom*

## Abstract

In this paper, a novel beta parameter three-input one-output fuzzy-logic based maximum power point tracking (MPPT) algorithm is presented for the photovoltaic (PV) system application. The conventional fuzzy-logic controllers (FLCs) exhibit obvious limitations such as their dependence on the user's knowledge about the system and complicated rules. Furthermore, they show inherent dilemma between the rules number of FLC and the universality for various operating conditions, which is revealed and explained with details in this paper. Thus, a novel FLC is proposed by introducing a third input: an intermediate variable  $\beta$ . It can simplify the fuzzy rule membership functions and cover wider operating conditions. The dependence on the user's knowledge about the system is reduced. The converging speed for transients is improved and oscillations around the MPPs are completely eliminated compared with conventional MPPT methods. Typical operation

\*Corresponding author

Email addresses: X.Li31@liverpool.ac.uk, Xingshuo.Li@xjtlu.edu.cn  
(Xingshuo Li), Huiqing.Wen@xjtlu.edu.cn (Huiqing Wen), Y.Hu35@liverpool.ac.uk  
(Yihua Hu), L.Jiang@liverpool.ac.uk (Lin Jiang)

conditions such as varying solar irradiation and load resistance are tested for fair comparison of various algorithms. An experimental prototype was designed and main experimental results were presented to verify the advantages of the proposed algorithm.

*Keywords:* photovoltaic (PV) system, Maximum power point tracking (MPPT), fuzzy logic controller(FLC), beta parameter, zero oscillation.

1        Since the output power of a PV system shows strong nonlinearity  
 2        with respect to the irradiation and temperature, the maximum power  
 3        point tracking (MPPT) techniques are usually adopted in the PV  
 4        system to achieve the maximum power output from the installed PV mod-  
 5        ules under different conditions (Elgendi et al., 2015).

6        So far, many MPPT techniques have been used (Esram and Chap-  
 7        man, 2007; Subudhi and Pradhan, 2013; de Brito et al., 2013), such as Perturb  
 8        and observe (P&O) (Femia et al., 2005; Elgendi et al., 2015), Hill-Climbing  
 9        (HC) (Kjaer, 2012) and incremental conductance (INC) (Safari and Mekhilef,  
 10       2011; Elgendi et al., 2013). However, these techniques show obvious disad-  
 11       vantages, such as low tracking efficiency during rapidly changing solar irra-  
 12       diation and fluctuations around the maximum power points (MPPs) during  
 13       the steady-state operation (Soon and Mekhilef, 2014).

14       In order to improve the performance, many advanced MPPT algorithms  
 15       have been proposed, such as the adaptive hill climbing (Xiao and Dunford,  
 16       2004), variable-step-size incremental conductance (Liu et al., 2008), and in-  
 17       cremental resistance (Mei et al., 2011), have been proposed. However, the  
 18       dilemma between the steady state and transient operations has not been  
 19       solved perfectly (Xiao and Dunford, 2004). The control implementation be-

comes complicated (Mei et al., 2011). Additional parameters such as scaling factor are introduced and the optimal parameter must be determined firstly to ensure good performance (Liu et al., 2008). Furthermore, there are still steady-state oscillations that could not be completely eliminated with these techniques.

In recent years, a number of MPPT algorithms without the determination of step size have been proposed to allocate the MPP. In (Teng et al., 2016), the weighted least square (WLS) function is used to determine the MPP with three sampled points. Similarly, two different polynomial models are used to fit the *I-V* curve and obtain the MPP with three sampled points (Blanes et al., 2013) and six sampled points (Zadeh and Fathi, 2017), respectively. However, these model-based MPPT methods have special requirements for the sampled points as well as a high computational burden to obtain the MPP. Alternatively, a thermography-based MPPT method (Hu et al., 2014) and a optical-camera-based MPPT method (Mahmoud and El-Saadany, 2017) are proposed to allocate the MPP. However, all these methods require additional hardware, which increases the system cost.

Compared with aforementioned MPPT algorithms, Fuzzy-logic controllers (FLCs) does not require any additional hardware and can be easily adapted to the existing PV systems(Yilmaz et al., 2018). Besides, it can also exhibit faster tracking speed and more accurate steady-state performance (Simoes and Franceschetti, 1999; Kottas et al., 2006). However, the conventional FLCs are heavily relied on the user's knowl-

edge about the PV system and their rules are complicated (Radjai et al., 2014). Furthermore, FLC could not track the real MPPs when the irradiation changes quickly (Alajmi et al., 2011). In order to overcome these drawbacks in FLC implementation, many researchers try to optimize the FLCs such as their membership functions (MFs) and fuzzy rules with the aid of the other artificial intelligence (AI) techniques, such as fuzzy cognitive networks (Kottas et al., 2006), genetic algorithm (Messai et al., 2011a), artificial neural network (Chaouachi et al., 2010), particle swarm optimization (Letting et al., 2012) and adaptive network-based fuzzy inference system(Abu-Rub et al., 2013). These AI techniques require designers deep knowledge in the practical implementation, which hinder the wide-use of these advanced FLC techniques.

To address this issue, a practical way is to combine the classical MPPT techniques, such as HC technique (Alajmi et al., 2011),P&O technique (Mohd Zainuri et al., 2014) and INC technique (Radjai et al., 2014) with the FLCs in order to achieve easier MFs and fuzzy rules design. With the hybrid technique, faster converging speed for transients and less oscillation around the MPPs for the steady-state operation can be achieved (Li and Wen, 2016). The design of the FLC is simplified, for instance, the number of fuzzy rules can be reduced from 25 to 16 (Alajmi et al., 2011). However, there is a dilemma between the rules number and the universality for various operating conditions. When the rules is simplified, the FLC will not track the MPPs successfully for some operating conditions. Thus, a balance between the complexity of the rules and the universality of the algorithm must be achieved.

70 This paper will follow the principle of the hybrid MPPT techniques by  
 71 introducing a variable  $\beta$  rather than the variation of the terminal voltage  
 72 or the output power as the third input of FLC. It simplifies the fuzzy rule  
 73 number and cover wider operating conditions. Both the static and dynamic  
 74 performance can be improved. A PV system connected with boost converter  
 75 was designed and the new FLC algorithm was implemented by the dSPACE.  
 76 Simulation and experimental results for different scenarios are presented to  
 77 demonstrate the advantages of the proposed MPPT algorithm in terms of  
 78 fast converging speed and zero oscillation.

## 79 **1. Conventional FLC MPPT Techniques**

80 Fig. 1 shows the basic structure of FLCs, which are usually implemented  
 81 with three stages: fuzzification, interference with rule base, and defuzzifica-  
 82 tion (Esram and Chapman, 2007). Main function of the fuzzification is to  
 83 convert the numerical input variables into equivalent linguistic variables as  
 84 input fuzzy sets. The input fuzzy sets are then sent to the interference in  
 85 order to obtain output fuzzy sets according to the fuzzy rule base table. Fi-  
 86 nally, the output of numerical variables can be obtained based on the output  
 87 fuzzy sets.

88 For MPPT application, FLCs usually use Mamdani model for interfer-  
 89 ence, Max-Min for fuzzy combination and center of gravity (COG) for de-  
 90 fuzzification. The variations of the duty cycle ( $\Delta D$ ) is the output variable.  
 91 The input variables are changed according to different FLC-based MPPT  
 92 techniques. Normally, the error  $E$  and the change in error  $\Delta E$  are acted as  
 93 the input variables (Esram and Chapman, 2007). The error  $E$  can be

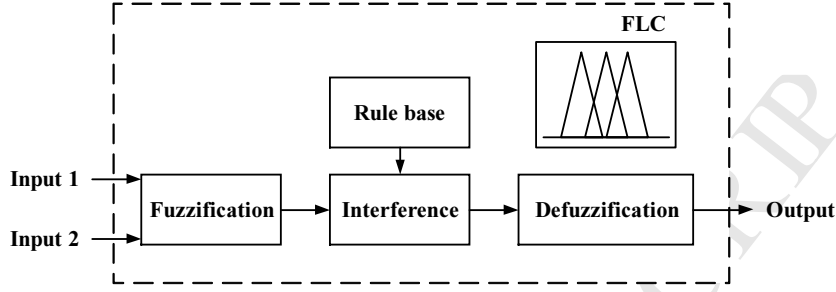


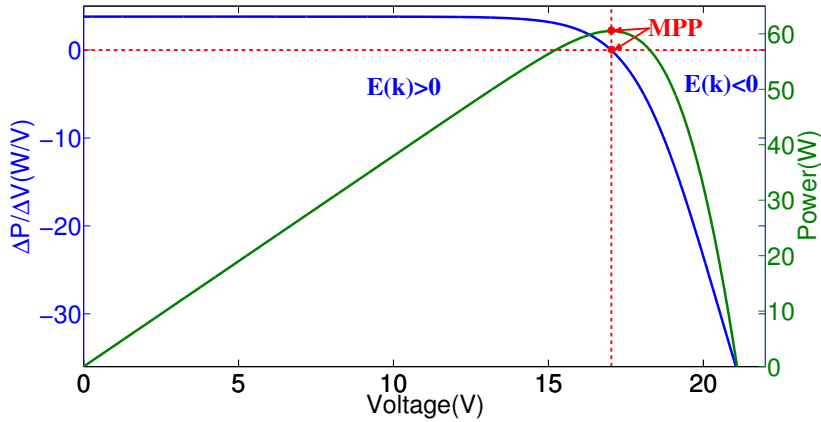
Fig. 1: Fuzzy logic controller.

94 obtained by the slope of P-V curve as follow(Messai et al., 2011b; Algazar  
95 et al., 2012):

$$E(k) = \frac{P(k) - P(k-1)}{V(k) - V(k-1)} \quad (1)$$

$$\Delta E(k) = E(k) - E(k-1) \quad (2)$$

96 where  $P(k)$  and  $V(k)$  represent the PV output power and voltage respectively  
97 at the time instant  $k$ . Fig. 2 indicates that the instantaneous value of  $E(k)$   
98 is positive on the left or negative on the right of the MPP.  
99

Fig. 2: Typical PV  $P$ - $V$  and  $\Delta P/\Delta V$  curves.

100 Normally the MFs of FLC-based MPPT techniques adopt five-

101 fuzzy-level structure, including NB (negative big), NS (negative  
 102 small), ZE (zero), PS (positive small), and PB (positive big). Since  
 103 the curve of  $\Delta P/\Delta V$  in Fig. 2 is highly asymmetric at the MPP,  
 104 the MFs of  $E(k)$  with five fuzzy levels have to be carefully de-  
 105 signed in order to ensure the symmetry of the output variable  $\Delta D$   
 106 (El Khateb et al., 2014). The designed MFs with five fuzzy levels  
 107 are demonstrated in Fig. 3, which shows that the output variable  
 108  $\Delta D$  is symmetric at zero. The number of fuzzy rules is 25, which  
 109 is high and will increase the difficulty of FLC design and imple-  
 110 mentation. Although some artificial intelligence (AI) algorithms  
 111 including fuzzy cognitive networks, genetic algorithm and particle  
 112 swarm optimization can be used to optimize the MFs and fuzzy  
 113 rules, these AI techniques themselves are complicated and require  
 114 designers deep knowledge for these advanced AI algorithms.

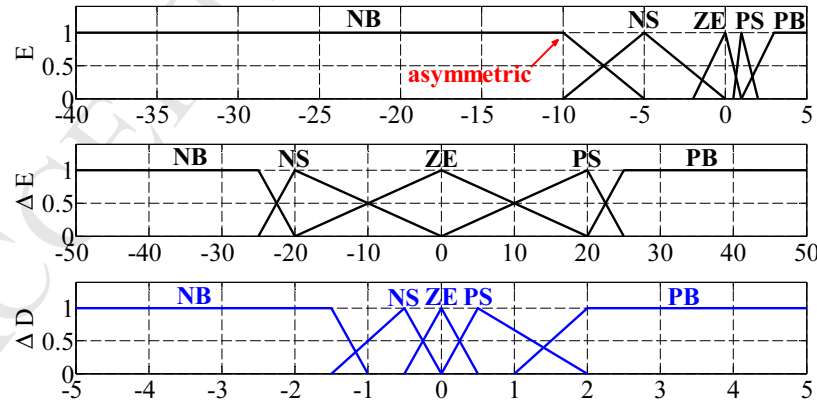


Fig. 3: Membership functions of five fuzzy levels.

115 Alternatively, some researchers try to integrate some classical MPPT

116 techniques with the conventional FLC in order to achieve simple design of  
 117 MFs and fuzzy rules. For instance, originated from the HC MPPT method,  
 118 the research in (Alajmi et al., 2011) utilizes the variation of the output power  
 119 ( $\Delta P$ ) and the variation of the output current ( $\Delta I$ ), instead of  $E$  and  $\Delta E$ , as  
 120 the input variables. Since this technique combines the HC with the fuzzy logic  
 121 MPPT technique, it is called fuzzy-logic-based hill-climbing (FLC-HC). Sim-  
 122 ilar hybrid MPPT algorithms, such as fuzzy-logic-based perturb and observe  
 123 (FLC-P&O) and fuzzy-logic-based incremental conductance (FLC-INC) can  
 124 be found in (Mohd Zainuri et al., 2014) and (Radjai et al., 2014), respec-  
 125 tively. In (Mohd Zainuri et al., 2014), the incremental conductance  $e_{IC}$  is  
 126 used for one of the input variables. These FLC techniques are summarised  
 127 in Table 1.

128 The comparison is made among these MPPT algorithms in terms of the  
 129 converging speed, steady oscillations, and the complexity in FLC implemen-  
 130 tation. For example, the method in (Alajmi et al., 2011) can reduce the  
 131 number of fuzzy rules from 25 to 16. Using three fuzzy levels, such as small,  
 132 medium and large, the method proposed in (Radjai et al., 2014; Al Nabulsi  
 133 and Dhaouadi, 2012) will further reduces to nine rules. However, for FLC  
 134 algorithms, there is an inherent dilemma between the rules number and the  
 135 universality for various operating conditions. For some conditions, some FLC  
 136 algorithms show bad performance or even could not track the MPPs properly.  
 137 This problem will be discussed in this paper and the corresponding reasons  
 138 are explained properly. Furthermore, all these FLC algorithms shown in  
 139 Table 1 present significant steady oscillations.

Table 1: Summarisation of the conventional FLC techniques.

Ref.	Input variables	Output variables	Number of Rules	Inference mode	Converter type	Controller implementation
Alajmi et al. (2011)	$\Delta P, \Delta I$	$\Delta D$	16	Mandani	Boost	Microchip Infineon TCI796
Mohd Zainuri et al. (2014)	$\Delta P, \Delta V$	$\Delta D$	25	Mandani	Boost	DSP TMS320F28335
Radjai et al. (2014)	$e_{IC}, \Delta D$	$\Delta D$	9	Mandani	Cuk	dSPACE
Messai et al. (2011b)	$\Delta P/\Delta V$	$\Delta D$	25	Mandani	Boost	FPGA V2MB1000
Algazar et al. (2012)	$\Delta P/\Delta V$	$\Delta D$	25	Mandani	Cuk	-
Al Nabulsi and Dhaouadi (2012)	$\Delta P/\Delta V, \Delta D$	$\Delta D$	9	Mandani	Buck	DSP TMS320F28335

<sup>140</sup> **2. Proposed Beta-Parameter based FLC MPPT Algorithm**

<sup>141</sup> *2.1. Proposed scheme for the single peak tracking*

<sup>142</sup> Fig. 4 shows the basic structure of the proposed algorithm. The Mamdani  
<sup>143</sup> model, Max-Min and COG are used for interference, fuzzy combination and  
<sup>144</sup> defuzzification, respectively. Besides the variation of the output power ( $\Delta P$ )  
<sup>145</sup> and the variation of the output voltage ( $\Delta V$ ), a third input variable  $\beta$  is  
<sup>146</sup> introduced. The variation of the duty cycle is the output.

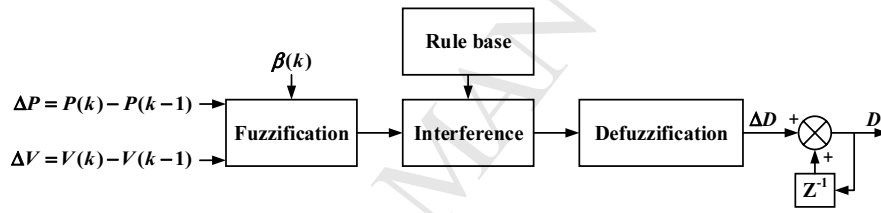


Fig. 4: Proposed FLC Algorithm.

Table 2: Values of  $\beta$  under various working conditions

No.	Irradiance	temperature	$\beta$
1	1000 W/m <sup>2</sup>	45°C	-15.4505
2	1000 W/m <sup>2</sup>	5°C	-18.3431
3	300 W/m <sup>2</sup>	45°C	-15.9587
4	300 W/m <sup>2</sup>	5°C	-19.0214

<sup>147</sup> The beta-parameter based MPPT algorithm was proposed by (Jain and  
<sup>148</sup> Agarwal, 2004) and the newly added variable  $\beta$  is expressed by:

$$\beta = \ln\left(\frac{I}{V}\right) - c \times V \quad (3)$$

149 where  $V$  and  $I$  represents the PV voltage and current,  $c$  is the function of  
 150 cell number, temperature, and the diode structure (Jain and Agarwal, 2004).

151 In this algorithm, a range of  $(\beta_{min}, \beta_{max})$  is defined, which depends on the  
 152 practical environmental conditions, such as the irradiance and temperature  
 153 (Li et al., 2016a). The parameter  $\beta$  is continuously monitored to determine  
 154 if it is located within the defined range. If  $\beta$  is located within this range, it  
 155 indicates that the operating point is close to the true MPP. Table 2 illustrates  
 156 the calculated magnitudes of  $\beta$  for different environmental conditions. **Fig. 5**  
 157 shows that the range of  $\beta$  is narrow for a wide range of working  
 158 conditions, which facilitates the dynamic tracking. In this paper  
 159 (Li et al., 2016b), two sets of the distinguished meteorological data  
 160 are used to validate the range of  $\beta$ . Generally, the range of  $\beta$  can  
 161 be easily determined by the local meteorological data under the  
 162 extreme conditions in terms of operating temperature and solar  
 163 irradiance.

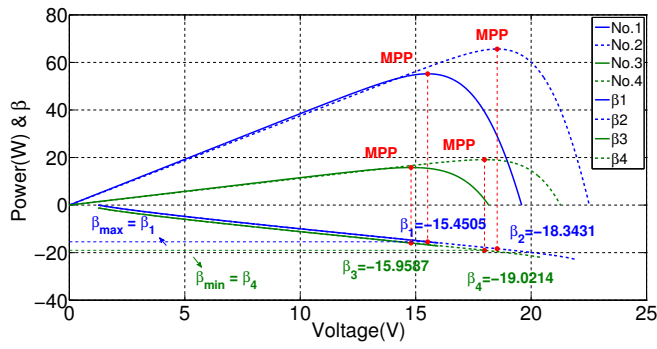


Fig. 5: Range of  $\beta$  and power under various irradiance and temperature conditions.

164 With the proposed algorithm, Fig. 6 and Table 3 shows the membership  
 165 functions and fuzzy rules. Three fuzzy sets,  $\beta_{min}$ ,  $\beta_{mid}$ , and  $\beta_{max}$ , are used

with respect to the variable  $\beta$ . Table 3 shows the fuzzy rules for the proposed MPPT technique. The output is either PB for  $\beta_{min}$  and or NB for  $\beta_{max}$  respectively, which is independent on the value of  $\Delta P$  and  $\Delta V$ . For  $\beta_{mid}$ , there are three possible fuzzy subsets: NS, ZE, and PS. Thus, there are totally only 11 rules required for the proposed FLC algorithm, which is much less than other FLCs. Compared with the FLC-HC, it covers wider operating conditions. Furthermore, the output shows relatively symmetric feature, as illustrated in Fig. 6, which further simplify the algorithm implementation.

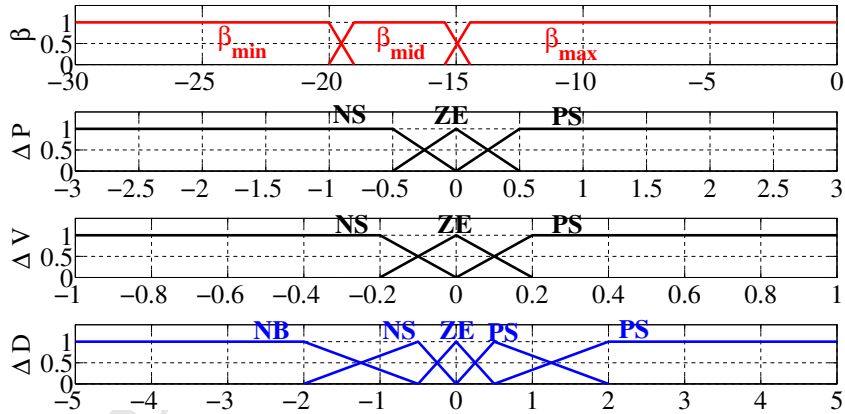


Fig. 6: MFs of the proposed FLC.

The detailed tracking process with the proposed algorithm is illustrated in Fig.7. The irradiance is set as follows: the irradiance is firstly set as  $1000 \text{ W/m}^2$ . At  $t=0.5 \text{ s}$ , the irradiance decreases to  $400 \text{ W/m}^2$ . The movement of the operating point can be explained as: firstly, the PV module operates at point A, which is the MPP for  $1000 \text{ W/m}^2$ , as shown in Fig.7 (a). At this time, the fuzzy input parameter  $\beta$  is  $\beta_{mid}$  and the other input parameters,  $\Delta P$  and  $\Delta V$ , are ZE. According to Table 3, the output  $\Delta D$  is ZE as shown

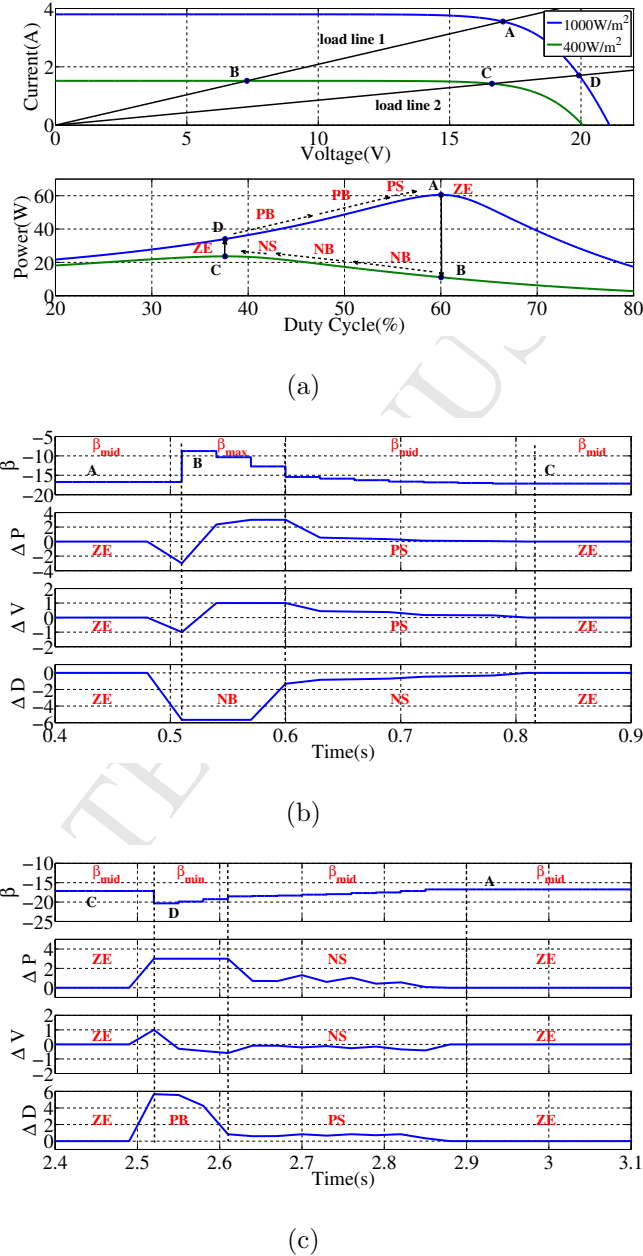


Fig. 7: Dynamic tracking process with the proposed FLC. (a)I-V and P-D curves; (b)Fuzzy parameters for the proposed technique when the irradiance decreases; (c)changes of the fuzzy parameters for the proposed technique when the irradiance increases.

Table 3: Fuzzy rules of the proposed FLC

$\beta_{min}$	PB			
$\beta_{mid}$	$\Delta V$	NS	ZE	PS
	$\Delta P$	NS	ZE	PS
	ZE	ZE	ZE	ZE
	PS	PS	ZE	NS
	NB			

in Fig.7 (b). For the irradiance change at  $t = 0.5s$ , the operating point will still locate at the load line 1 considering that the duty cycle of the power converter remains unchanged at that moment. Specifically, the operating point switches immediately from A to B, which is the intersection point between the load line 1 and the I-V curve for  $400 \text{ W/m}^2$ . Then,  $\beta$  is found as  $\beta_{max}$ , so  $\Delta D$  is NB regardless of  $\Delta P$  and  $\Delta V$  according to Table 3. At  $t = 0.6s$ ,  $\beta$  is equal to  $\beta_{mid}$  and both of  $\Delta P$  and  $\Delta V$  are equal to PS, as illustrated in Fig.7 (b). Consequently,  $\Delta D$  is equal to NS. After several iteration, both of  $\Delta P$  and  $\Delta V$  are equal to ZE, so  $\Delta D$  is stabilized to ZE. Thus, point C is finally located for the steady state operation and the zero oscillation is realized. Fig.7 (c) illustrates the case for the irradiance increase, which shows similar process.

### 2.2. Multiple peaks tracking under partial shading conditions

In practice, a PV string (or a PV array) rather than a PV module is generally used. When the PV string is partially shaded, there will be multiple peaks rather than a single peak for its correspond-

197 ing  $I$ - $V$  curve. Some MPPT methods may be affected since these  
 198 MPPT methods are unable to distinguish the global MPP (GMPP)  
 199 from the local MPPs (LMPPs). However, the proposed method  
 200 can be easily extended for the multiple-peak tracking. The key in  
 201 the algorithm implementation is how to convert one multiple-peak  
 202 curve into several single-peak curves (Li et al., 2018).

203 In (Batzelis et al., 2014, 2015), it was pointed out the  $I$ - $V$  curve  
 204 of a PV string is always determined by one key module since other  
 205 modules are approximately constant or linear function. Therefore,  
 206 an explicit functions of the equivalent values of voltage ( $V_{eq}$ ) of this  
 207 key module is expressed as (Li et al., 2018):

$$V_{eq} = V_{String} - (n - 1) \times V_s + (m - n) \times V_d \quad (4)$$

$$V_s \approx \frac{V_{MPP,stc} - V_{oc,stc}}{I_{MPP,stc}} \times I_{String} + V_{oc,stc} \quad (5)$$

$$n = 1, 2 \dots m, \text{for } (m - 1) \cdot \alpha \cdot V_{oc} < V_{String} \leq m \cdot \alpha \cdot V_{oc} \quad (6)$$

210 where  $V_{String}$  and  $I_{String}$  represent the output voltage and current of  
 211 the PV string, respectively;  $V_d$  refers to the constant value while  
 212  $V_s$  refers to the linear source as expressed in (5);  $m$  refers to the  
 213 total number of PV modules in the PV string, and  $n$  is determined  
 214 by (6);  $V_{oc}$  is the open-circuit voltage of PV modules,  $V_{MPP,stc}$  and  
 215  $I_{MPP,stc}$  represent the voltage and current at the MPP under the  
 216 standard test condition (STC), respectively;  $\alpha$  is a variable that is  
 217 varying from 0.8 to 0.97 (Ahmed and Salam, 2015).

218 Substitute (4-6) into (3), the equivalent value of  $\beta$ ,  $\beta_{eq}$ , can be  
 219 determined. As a consequence, the  $I$ - $V$  curves for the PV string

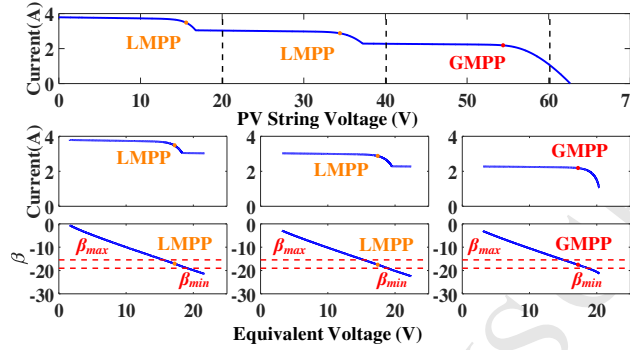


Fig. 8: *I-V* curves for the PV string with the multiple peaks and its equivalent values of voltage and  $\beta$ .

with the multiple peaks and its equivalent values of voltage and  $\beta$  are shown in Fig.8. As shown in Fig.8, the whole *I-V* curves for the PV string is converted into three single-peak curves. Then, the each single-peak curve can be individually tracked by the proposed method and the possible extensions of the proposed method is shown in Fig.9.

As shown in Fig.9, the proposed method, such as membership functions and fuzzy rules, is remained. One of the input parameter for the proposed method,  $\beta(k)$ , is changed to  $\beta_{eq}(k)$ , which is determined by (4-6). The step size generated by the proposed method  $\Delta D_1$  is used to track each single-peak curve and the step size generated by the search mode  $\Delta D_2$  is used to move the operating point from one peak to another. Finally, the decision block decides to new step size is  $\Delta D_1$  or  $\Delta D_2$ . The details related to the search mode and decision block could be found in (Li et al., 2018). The research focus of this paper is to validate the effectiveness of

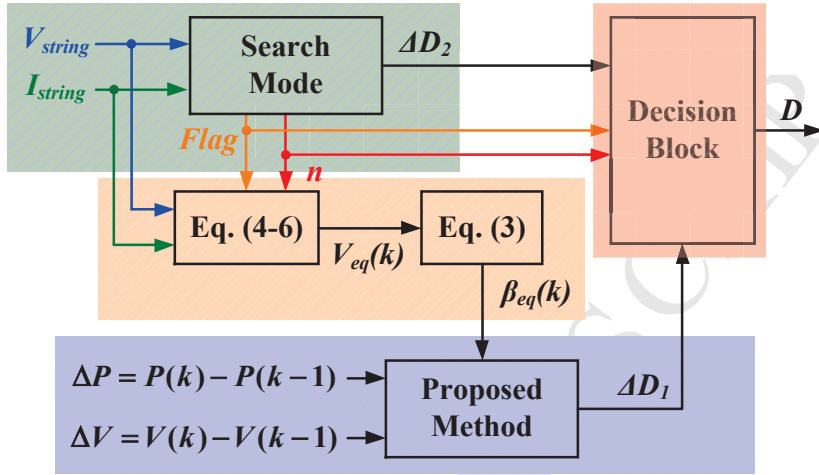


Fig. 9: Possible extensions of the proposed method for the multiple-peak tracking.

236 the proposed Beta parameter-based fuzzy-logic control under the  
 237 uniform irradiation conditions through simulation and experiments  
 238 since the proposed algorithm can be easily changed to adapt to  
 239 the partial shading conditions.

### 240 3. Simulation Analysis

241 Fig.10 shows the simulation model with main components such as the PV  
 242 module, boost converter with the proposed FLC and load. Main parameters  
 243 for the PV modules, MSX-60W are: maximum power is 60 W, the voltage  
 244 and current at the maximum power are 17.1 V and 3.5 A, open-circuit voltage  
 245 is 21.1 V, and the short-circuit current is 3.8 A. Table 4 lists main parameters  
 246 for the boost converter. The MatLab/Simulink sub-model for the proposed  
 247 MPPT technique is shown in Fig.11. The sampling time for the MPPT  
 248 algorithm,  $T_p$ , is set as 0.03 s.

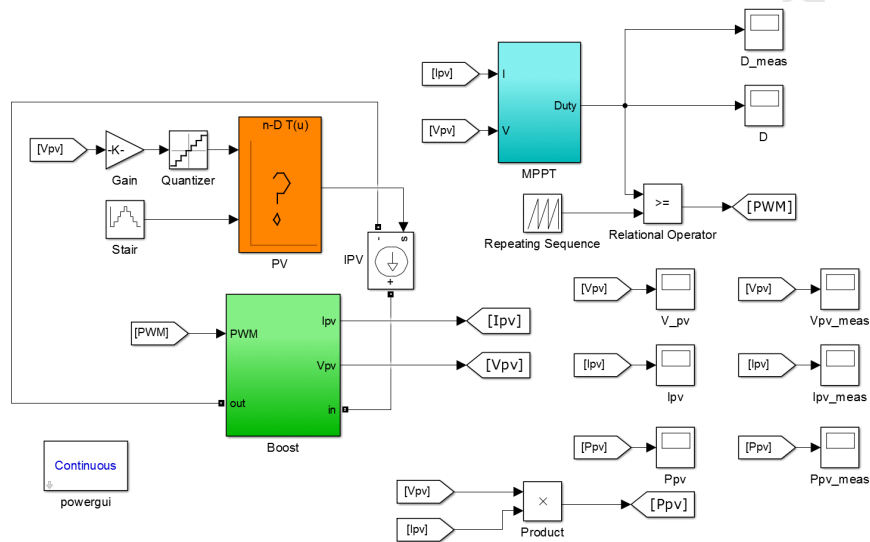


Fig. 10: Simulation model of PV system with MPPT control in MatLab/Simulink

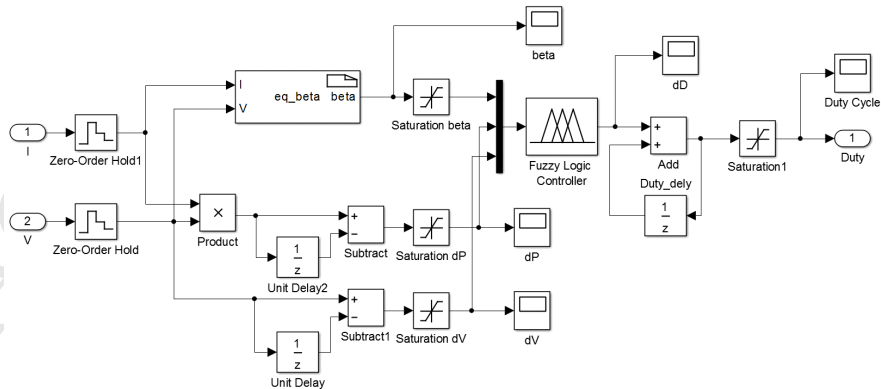


Fig. 11: Proposed MPPT technique with FLC in MatLab/Simulink.

Table 4: Main Parameters of the boost converter

Parameter	Symbol	Value
PV side input capacitance	$C_{in}$	470 uF
Output capacitance	$C_{out}$	47 uF
Inductance	$L$	1 mH
Switching frequency (IGBT)	$f_{sw}$	10 kHz

249 In order to comprehensively evaluate the performance of the proposed  
 250 technique, typical MPPT techniques such as P&O technique (Femia et al.,  
 251 2005), FLC-HC technique (Alajmi et al., 2011), and the proposed algorithm  
 252 are tested. Three different scenarios are considered, including the strong-  
 253 intensity irradiance change, the weak-intensity irradiance change, and the  
 254 load change.

255 *3.1. Scenario One: Strong-intensity irradiance change*

256 The scenario of strong-intensity irradiance change is defined that the irra-  
 257 diance changes between  $1000W/m^2$  and  $600W/m^2$ . At  $t=0.5$  s, the irradiance  
 258 level is decreased to  $600 W/m^2$ . At  $t=2$  s, it will return back to  $1000 W/m^2$   
 259 . For this scenario,  $R_{load}$  is fixed at  $30 \Omega$ .

260 Fig.12 shows main simulation results. It indicates that P&O needs longest  
 261 time to find the true MPPT and then followed by the FLC-HC algorithm.  
 262 The steady-state oscillations with both algorithm can be easily observed.  
 263 Thus, the static power loss is increased. Besides, Fig.12 (b) shows that  
 264 the FLC-HC shows the divergence from the real MPP when the irradiance  
 265 decreases. The proposed FLC takes the shortest time among the three algo-

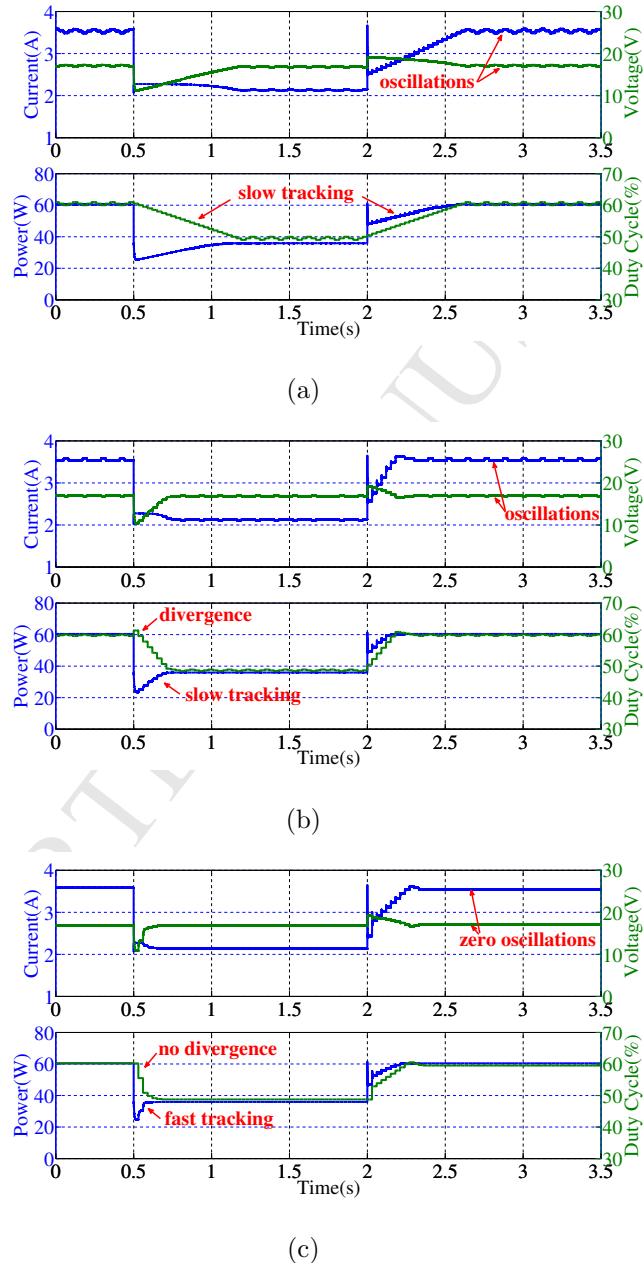


Fig. 12: Simulation results for the Scenario One. (a)P&O technique; (b)FLC-HC technique; (c)the proposed technique.

266      rithms. Furthermore, Fig.12 (c) shows no divergence and zero steady-state  
 267      oscillation.

268      *3.2. Scenario Two: Weak-intensity irradiance change*

269      The scenario of strong-intensity irradiance change is defined that the irra-  
 270      diance changes between  $400 \text{ W/m}^2$  and  $100 \text{ W/m}^2$ . At  $t=1 \text{ s}$ , the irradiance  
 271      level is decreased to  $100 \text{ W/m}^2$ . At  $t=4 \text{ s}$ , it will return back to  $400 \text{ W/m}^2$ .  
 272      For this scenario,  $R_{load}$  is fixed at  $80 \Omega$ , which represents low-power operating  
 273      region.

274      Fig.13 shows main simulation results. Among these algorithms, the pro-  
 275      posed technique requires shortest time to find the real MPP. Fig.13 (b) indi-  
 276      cates that FLC-HC technique could not find the real MPP for this scenario  
 277      with  $100 \text{ W/m}^2$  irradiance. This can be explained by the detailed tracking  
 278      process of FLC-HC algorithm, which is shown in Fig.14. At time  $t = 1 \text{ s}$ , the  
 279      irradiance decreases from  $400 \text{ W/m}^2$  to  $100 \text{ W/m}^2$  and the operating point  
 280      moves from point E to F. Since both of  $\Delta P$  and  $\Delta I$  are NB,  $\Delta D$  is equal to  
 281      PB according to the rule table of **FLC-HC (Alajmi et al., 2011)**. How-  
 282      ever, this results in the divergence from the MPP, as illustrated in Fig.14.  
 283      Furthermore, since the point F is located around the  $I_{sc}$ , both of  $\Delta P$  and  
 284       $\Delta I$  are always NS. Therefore, the output  $\Delta D$  is always equal to NS, which  
 285      results in a slow tracking speed (Alajmi et al., 2011).

286      *3.3. Scenario Three: Load change*

287      This scenario is defined that  $R_{load}$  changes between  $60 \Omega$  and  $30 \Omega$ . At  
 288       $t=0.5 \text{ s}$ ,  $R_{load}$  is decreased to  $30 \Omega$ . At  $t=2 \text{ s}$ , it will return back to  $60 \Omega$ .  
 289      During this period, the irradiance is fixed at  $600 \text{ W/m}^2$ .

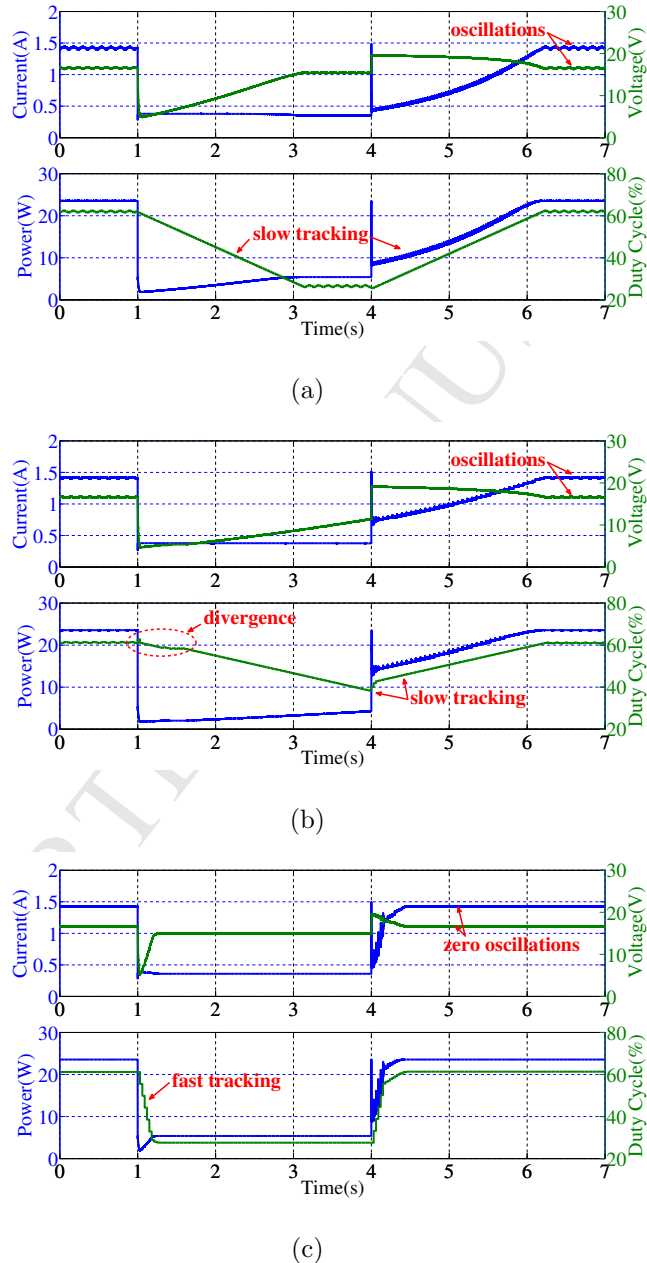


Fig. 13: Simulation results for the Scenario Two. (a)P&O technique; (b)FLC-HC technique; (c)the proposed technique.

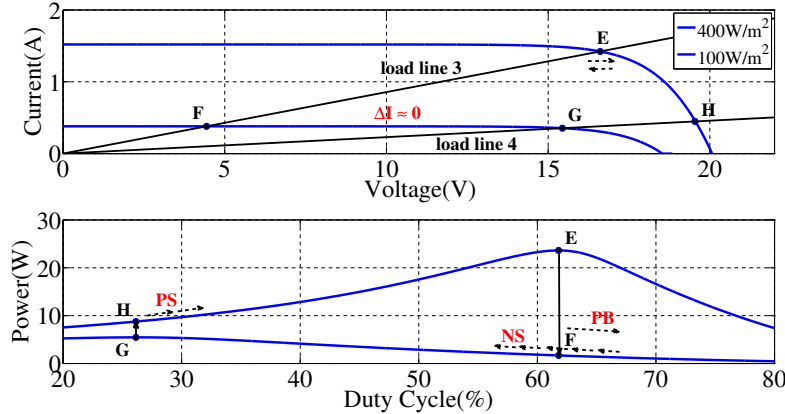


Fig. 14: Simulation results by using the FLC-HC technique.

290 Fig.15 shows main simulation results. Fig.15 shows that the proposed  
 291 FLC requires least time to determine the real MPP while P&O requires  
 292 longest time, as shown in Fig.15. This conclusion is similar with that of  
 293 previous two scenarios. Furthermore, Fig.12 shows no divergence and zero  
 294 static oscillations.

#### 295 4. Experimental Results

296 Experimental tests on a **prototype** were conducted in order to verify  
 297 the advantages of the proposed FLC. Fig.16 shows the test bench of this  
 298 PV system, including main components such as PV emulator Chroma ATE-  
 299 62050H-600S, boost converter, dSPACE DS1104 controller, and electronic  
 300 load IT8514C+. The parameters of boost converter **were** set the same as  
 301 the simulation. Three scenarios were evaluated and their parameter setting  
 302 was set the same as the simulation.

303 Fig.17 shows main experimental waveforms, **including** the output power,

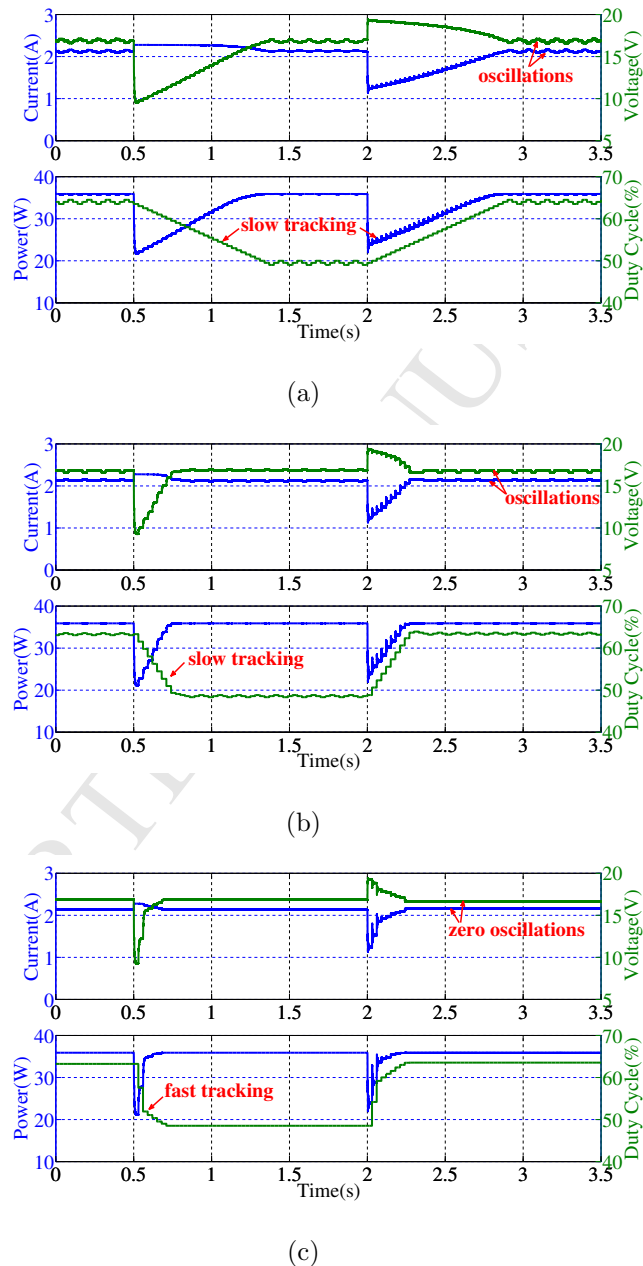


Fig. 15: Simulation results for the Scenario Three. (a)P&O technique; (b)FLC-HC technique; (c)the proposed technique.

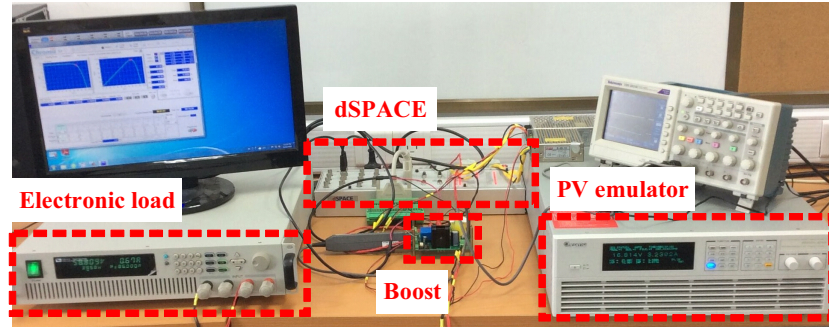


Fig. 16: Experimental prototype.

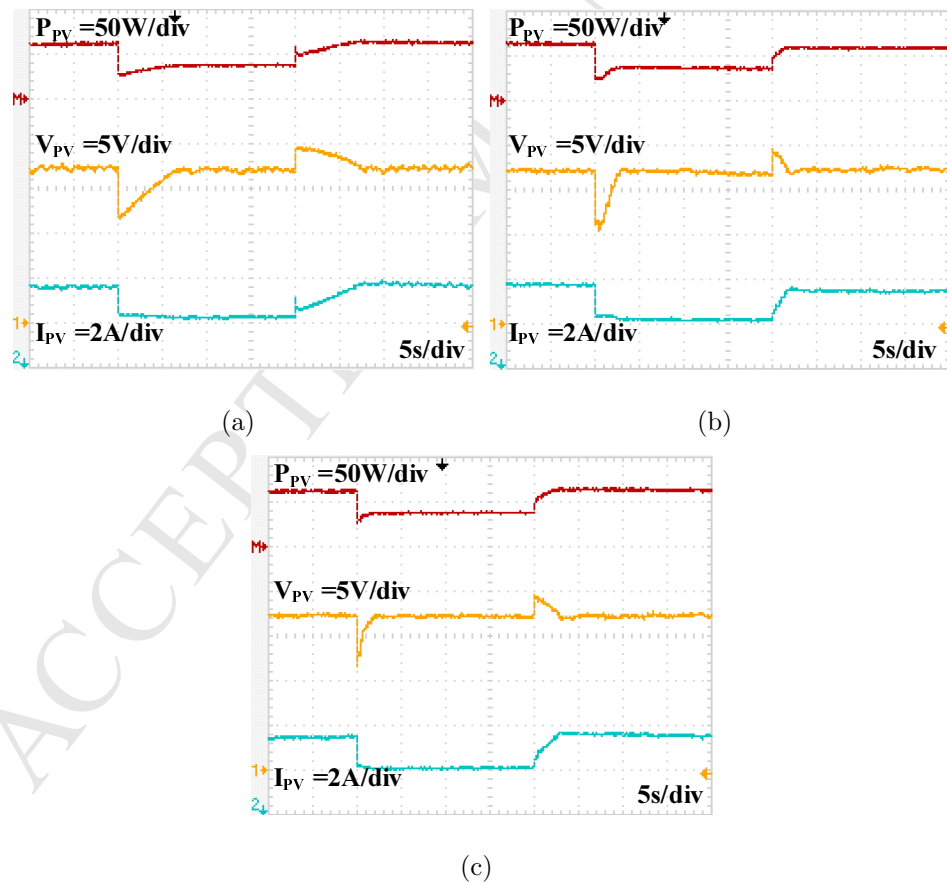


Fig. 17: Experimental results for the Scenario One. (a)P&amp;O technique; (b)FLC-HC technique; (c)the proposed technique.

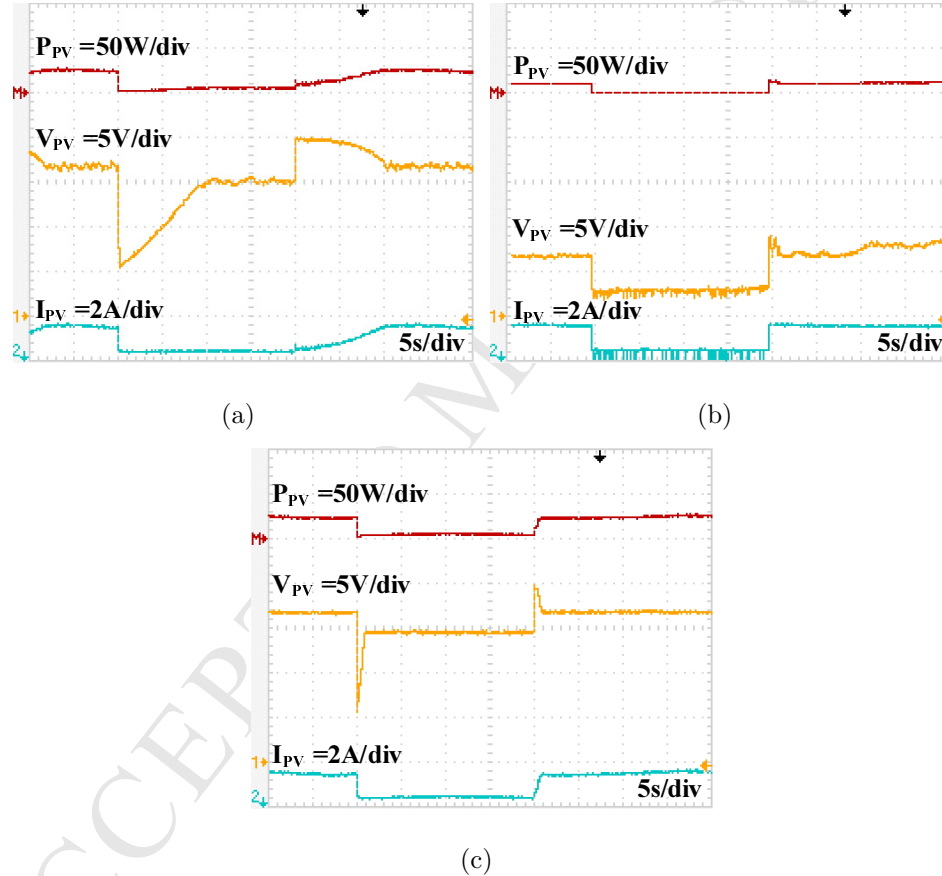


Fig. 18: Experimental results for the Scenario Two. (a)P&O technique; (b)FLC-HC technique; (c)the proposed technique.

304 current and voltage from the PV emulator under the Scenario One. It shows  
 305 that the proposed FLC requires the least time to determine the real MPP  
 306 among all these three algorithms. No steady oscillations were observed with  
 307 the proposed FLC while the steady-static oscillations with other algorithms  
 308 are easily observed.

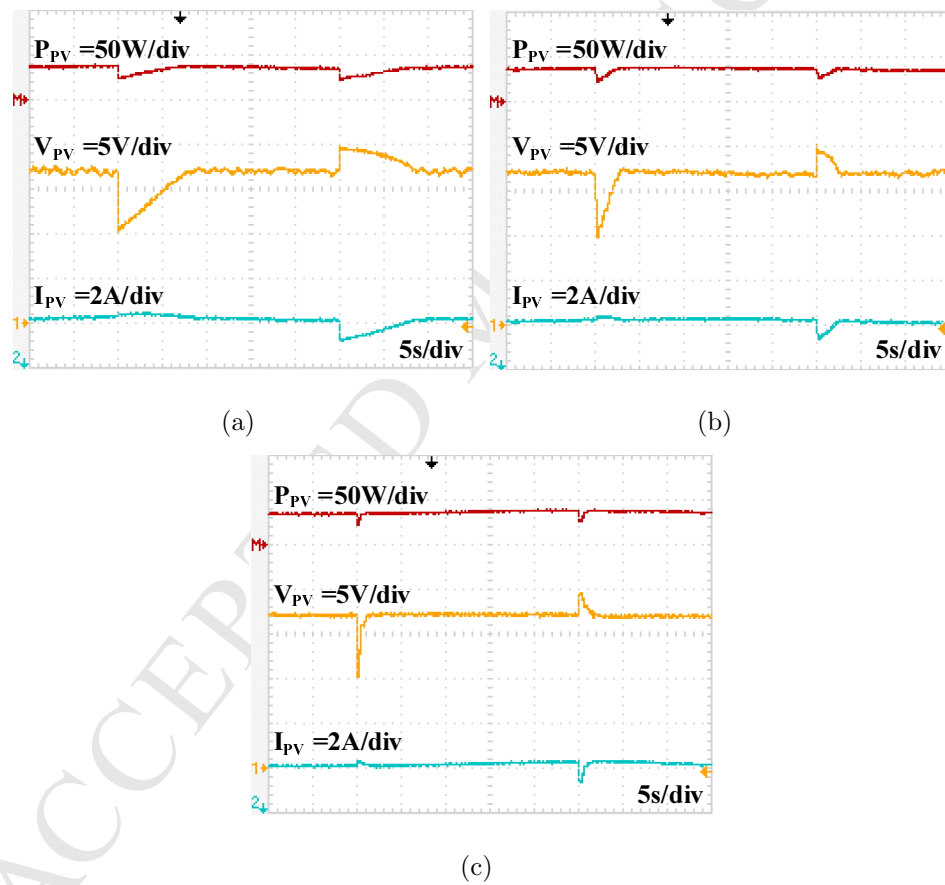


Fig. 19: Experimental results for the Scenario Three. (a)P&O technique; (b)FLC-HC technique; (c)the proposed technique.

309 Fig.18 shows the experimental results for the Scenario Two. The pro-  
 310 posed FLC exhibits the least tracking time, the lowest tracking power loss,

311 and zero oscillations among these MPPT techniques. The FLC-HC technique  
 312 is unable to track the MPP under this scenario and the PV voltage could  
 313 not reach the new steady state due to the irradiation variation, as illustrated  
 314 in Fig.18(b). Obvious oscillation in voltage and current waveforms are ob-  
 315 served. This phenomenon that FLC-HC could not track the MPP under low  
 316 irradiation conditions has been explained in Fig.14 of section VI. For the  
 317 P&O technique, the static voltage oscillations are easily observed especially  
 318 for the low irradiance condition of  $100 \text{ W/m}^2$ .

319 Fig.19 illustrates the experimental results for the Scenario Three. The  
 320 proposed FLC shows faster responses than the other methods and zero os-  
 321 cillate for the steady-state operation.

## 322 5. Conclusion

323 This paper proposed a novel FLC MPPT algorithm with  $\beta$  parameter.  
 324 It's new three-inputs one-output fuzzy-logic controller by introducing an in-  
 325 termediate variable  $\beta$  as the input variable. The dilemma between the rules  
 326 number and the universality for various operating conditions can be effec-  
 327 tively solved with this new algorithm. It can simplify the Fuzzy rule mem-  
 328 bership functions since the number of fuzzy rules can be reduced to 11.  
 329 Furthermore, this algorithm can be used for various operating conditions es-  
 330 pecially for rapidly changing environmental conditions and low irradiation  
 331 conditions, where the FLC-HC could not track the real MPPs successfully.  
 332 The dependency of this method on the designer's knowledge of the system  
 333 is reduced by using the new algorithm since the intermediate variable  $\beta$  can  
 334 be directly calculated from the measured voltage and current for each sam-

pling period. The converging speed for transients is improved by comparison with other MPPT methods. Oscillations around the MPPs are completely eliminated for steady-state operations. Various scenarios are analyzed and simulated according to the irradiance change and load variation. Simulation and experimental results were provided, which verified the advantages of the proposed FLC algorithm.

### 341 Acknowledgment

342 This research was supported by University Research Development Fund  
 343 (RDF-16-01-10), the Suzhou Prospective Application Programme (SYG201723),  
 344 the Jiangsu Science and Technology Programme (BK20161252), and the Na-  
 345 tional Nature Science Foundation of China (51407145).

### 346 6. Reference

- 347 Abu-Rub, H., Iqbal, A., Moin Ahmed, S., Peng, F. Z., Yuan, L., Ge, B.,  
 348 2013. Quasi-z-source inverter-based photovoltaic generation system with  
 349 maximum power tracking control using anfis. IEEE Trans. Sustain. Energy  
 350 4 (1), 11–20.
- 351 Ahmed, J., Salam, Z., Dec. 2015. An improved method to predict the position  
 352 of maximum power point during partial shading for pv arrays. IEEE Trans.  
 353 Ind.l Informat. 11 (6), 1378–1387.
- 354 Al Nabulsi, A., Dhaouadi, R., Aug. 2012. Efficiency optimization of a dsp-  
 355 based standalone pv system using fuzzy logic and dual-mppt control. IEEE  
 356 Trans. Ind. Informat. 8 (3), 573–584.

- 357 Alajmi, B., Ahmed, K. H., Finney, S. J., Williams, B. W., Apr. 2011. Fuzzy-  
 358 logic-control approach of a modified hill-climbing method for maximum  
 359 power point in microgrid standalone photovoltaic system. *IEEE Trans.*  
 360 *Power Electron.* 26 (4), 1022–1030.
- 361 Algazar, M. M., Al-monier, H., El-halim, H. A., Salem, M. E. E. K., 2012.  
 362 Maximum power point tracking using fuzzy logic control. *Int. J. Elec.*  
 363 *Power* 39 (1), 21–28.
- 364 Batzelis, E. I., Kampitsis, G. E., Papathanassiou, S. A., Manias, S. N., Mar.  
 365 2015. Direct mpp calculation in terms of the single-diode pv model param-  
 366 eters. *IEEE Trans. Energy Convers.* 30 (1), 226–236.
- 367 Batzelis, E. I., Routsolias, I. A., Papathanassiou, S. A., Jan. 2014. An ex-  
 368 plicit pv string model based on the lambert w function and simplified mpp  
 369 expressions for operation under partial shading. *IEEE Trans. Sustain. En-*  
 370 *ergy* 5 (1), 301–312.
- 371 Blanes, J. M., Toledo, F. J., Montero, S., Garrigs, A., Mar. 2013. In-site real-  
 372 time photovoltaic i-v curves and maximum power point estimator. *IEEE*  
 373 *Trans. Power Electron.* 28 (3), 1234–1240.
- 374 Chaouachi, A., Kamel, R. M., Nagasaka, K., 2010. A novel multi-model  
 375 neuro-fuzzy-based mppt for three-phase grid-connected photovoltaic sys-  
 376 tem. *Sol. Energy* 84 (12), 2219–2229.
- 377 de Brito, M., Galotto, L., Sampaio, L., de Azevedo e Melo, G., Canesin,  
 378 C., Mar. 2013. Evaluation of the main mppt techniques for photovoltaic  
 379 applications. *IEEE Trans. Ind. Electron* 60 (3), 1156–1167.

- 380 El Khateb, A., Abd Rahim, N., Selvaraj, J., Uddin, M., Jul. 2014. Fuzzy-  
 381 logic-controller-based sepic converter for maximum power point tracking.  
 382 IEEE Trans. Ind. Appl. 50 (4), 2349–2358.
- 383 Elgendy, M., Zahawi, B., Atkinson, D., Jan. 2013. Assessment of the in-  
 384 cremental conductance maximum power point tracking algorithm. IEEE  
 385 Trans. Sustain. Energy 4 (1), 108–117.
- 386 Elgendy, M., Zahawi, B., Atkinson, D., Mar. 2015. Operating characteristics  
 387 of the p amp; o algorithm at high perturbation frequencies for standalone  
 388 pv systems. IEEE Trans. Energy Convers. 30 (1), 189–198.
- 389 Esram, T., Chapman, P., Jun. 2007. Comparison of photovoltaic array max-  
 390 imum power point tracking techniques. IEEE Trans. Energy Convers.  
 391 22 (2), 439–449.
- 392 Femia, N., Petrone, G., Spagnuolo, G., Vitelli, M., Jul. 2005. Optimization of  
 393 perturb and observe maximum power point tracking method. IEEE Trans.  
 394 Power Electron. 20 (4), 963–973.
- 395 Hu, Y., Cao, W., Wu, J., Ji, B., Holliday, D., Nov. 2014. Thermography-  
 396 based virtual mppt scheme for improving pv energy efficiency under partial  
 397 shading conditions. IEEE Trans. Power Electron. 29 (11), 5667–5672.
- 398 Jain, S., Agarwal, V., Mar. 2004. A new algorithm for rapid tracking of  
 399 approximate maximum power point in photovoltaic systems. IEEE Power  
 400 Electron. Lett. 2 (1), 16–19.

- 401 Kjaer, S., Dec. 2012. Evaluation of the hill climbing and the incremental con-  
 402 ductance maximum power point trackers for photovoltaic power systems.  
 403 IEEE Trans. Energy Convers. 27 (4), 922–929.
- 404 Kottas, T. L., Boutalis, Y. S., Karlis, A. D., Sep. 2006. New maximum power  
 405 point tracker for pv arrays using fuzzy controller in close cooperation with  
 406 fuzzy cognitive networks. IEEE Trans. Energy Convers. 21 (3), 793–803.
- 407 Letting, L. K., Munda, J. L., Hamam, Y., 2012. Optimization of a fuzzy  
 408 logic controller for pv grid inverter control using s-function based pso. Sol.  
 409 Energy 86 (6), 1689–1700.
- 410 Li, X., Wen, H., 2016. A fuzzy logic controller with beta parameter for max-  
 411 imum power point tracking of photovoltaic systems. In: 2016 IEEE 8th  
 412 International Power Electronics and Motion Control Conference (IPEMC-  
 413 ECCE Asia). pp. 1550–1555.
- 414 Li, X., Wen, H., Hu, Y., Jiang, L., Xiao, W., Mar. 2018. Modified beta  
 415 algorithm for gmppt and partial shading detection in photovoltaic systems.  
 416 IEEE Trans. Power Electron. 33 (3), 2172–2186.
- 417 Li, X., Wen, H., Jiang, L., Hu, Y., Zhao, C., Sep. 2016a. An improved beta  
 418 method with auto-scaling factor for photovoltaic system. IEEE Trans. Ind.  
 419 Appl. 52 (5), 4281–4291.
- 420 Li, X., Wen, H., Jiang, L., Xiao, W., Du, Y., Zhao, C., Nov. 2016b. An  
 421 improved mppt method for pv system with fast-converging speed and zero  
 422 oscillation. IEEE Trans. Ind. Appl. 52 (6), 5051–5064.

- 423 Liu, F., Duan, S., Liu, F., Liu, B., Kang, Y., Jul. 2008. A variable step  
 424 size inc mppt method for pv systems. IEEE Trans. Ind. Electron. 55 (7),  
 425 2622–2628.
- 426 Mahmoud, Y., El-Saadany, E. F., Mar. 2017. A novel mppt technique based  
 427 on an image of pv modules. IEEE Trans. Energy Convers. 32 (1), 213–221.
- 428 Mei, Q., Shan, M., Liu, L., Guerrero, J., Jun. 2011. A novel improved variable  
 429 step-size incremental-resistance mppt method for pv systems. IEEE Trans.  
 430 Ind. Electron 58 (6), 2427–2434.
- 431 Messai, A., Mellit, A., Guessoum, A., Kalogirou, S. A., 2011a. Maximum  
 432 power point tracking using a ga optimized fuzzy logic controller and its  
 433 fpga implementation. Sol. Energy 85 (2), 265–277.
- 434 Messai, A., Mellit, A., Massi Pavan, A., Guessoum, A., Mekki, H., 2011b.  
 435 Fpga-based implementation of a fuzzy controller (mppt) for photovoltaic  
 436 module. Energy Convers. Manage. 52 (7), 2695–2704.
- 437 Mohd Zainuri, M., Mohd Radzi, M., Soh, A., Rahim, N., 2014. Development  
 438 of adaptive perturb and observe-fuzzy control maximum power point track-  
 439 ing for photovoltaic boost dc-dc converter. IET Renew. Power Gen. 8 (2),  
 440 183–194.
- 441 Radjai, T., Rahmani, L., Mekhilef, S., Gaubert, J. P., 2014. Implementation  
 442 of a modified incremental conductance mppt algorithm with direct control  
 443 based on a fuzzy duty cycle change estimator using dspace. Sol. Energy  
 444 110, 325–337.

- 445 Safari, A., Mekhilef, S., Apr. 2011. Simulation and hardware implementation  
 446 of incremental conductance mppt with direct control method using cuk  
 447 converter. *IEEE Trans. Ind. Electron.* 58 (4), 1154–1161.
- 448 Simoes, M. G., Franceschetti, N. N., Sep. 1999. Fuzzy optimisation based  
 449 control of a solar array system. *IEE Proc. Electr. Power Appl.* 146 (5),  
 450 552558.
- 451 Soon, T. K., Mekhilef, S., 2014. Modified incremental conductance mppt  
 452 algorithm to mitigate inaccurate responses under fast-changing solar irra-  
 453 diation level. *Sol. Energy* 101 (0), 333 – 342.
- 454 Subudhi, B., Pradhan, R., Jan. 2013. A comparative study on maximum  
 455 power point tracking techniques for photovoltaic power systems. *IEEE*  
 456 *Trans. Sustain. Energy* 4 (1), 89–98.
- 457 Teng, J. H., Huang, W. H., Hsu, T. A., Wang, C. Y., Aug. 2016. Novel  
 458 and fast maximum power point tracking for photovoltaic generation. *IEEE*  
 459 *Trans. Ind. Electron.* 63 (8), 4955–4966.
- 460 Xiao, W., Dunford, W., Jun. 2004. A modified adaptive hill climbing mppt  
 461 method for photovoltaic power systems. In: *Proc. 2004 IEEE 35th Annu.*  
 462 *Power Electron. Spec. Conf.* Vol. 3. pp. 1957–1963 Vol.3.
- 463 Yilmaz, U., Kircay, A., Borekci, S., Jan. 2018. Pv system fuzzy logic mppt  
 464 method and pi control as a charge controller. *Renew. Sust. Energ. Rev.* 81,  
 465 994–1001.
- 466 Zadeh, M. J. Z., Fathi, S. H., Dec. 2017. A new approach for photovoltaic

- <sup>467</sup> arrays modeling and maximum power point estimation in real operating  
<sup>468</sup> conditions. IEEE Trans. Ind. Electron. 64 (12), 9334–9343.

**Highlights**

- A novel FLC is proposed by introducing a third input: an intermediate variable  $\beta$  and it can simplify the fuzzy rule membership functions and cover wider operating conditions.
- The dependency on the designer's knowledge of the system can be reduced by using the proposed algorithm.
- The converging speed for transients is improved and oscillations around the MPPs are completely eliminated compared with conventional MPPT methods.
- Various scenarios are analyzed and simulated according to the irradiance change and load variation.
- Both simulation and experimental evaluation demonstrate the superior performance over other traditional MPPT methods.